International Journal of Smart Grid (IJSmartGrid)
https://www.ijsmartgrid.org/ Online ISSN: 2602-439X
B. Tasdemir and M. Yaz, Vol. 10, No. 1, March, 2026 Research Article

Comparative Short-Term Wind Energy Forecasting Using Hybrid JAYA-ANN, GRU-ANN, and VMD-ANN Models

Bahtiyar Tasdemir*‡, Mustafa Yaz**

*Department of Electrical and Electronics Engineering, Yozgat Bozok University, Yozgat, Turkey

**Department of Electrical and Electronics Engineering, Yozgat Bozok University, Yozgat, Turkey

(bahtiyartasdemir1830@gmail.com, Mustafa.yaz@yobu.edu.tr)

‡Bahtiyar Tasdemir; Yozgat Bozok University, Yozgat, Turkey, Tel: +90 354 242 10 02,

Fax: +90 354 217 89 91, bahtiyartasdemir1830@gmail.com

Received: 21.11.2025 Accepted: 21.01.2026

Abstract- Wind power generation is directly dependent on weather conditions, so it is very difficult to predict how much energy will be generated in a given time period. The main objective of this study is to predict wind power generation more accurately by comparing an Artificial Neural Network (ANN)-based forecasting model with JAYA-ANN, Gated Recurrent Unit (GRU)-ANN, and Variational Mode Decomposition (VMD)-ANN hybrid models. Wind direction, particulate matter (PM10), temperature, and historical power data for summer and spring seasons were collected to estimate the daily wind power generation capacity. Of the collected data, 80% was divided into a training set, 10% into a validation set, and 10% into a test set, and appropriate modelling methods were applied. The performance of the models was evaluated with Mean Absolute Percentage Error (MAPE), Root Mean Squared Error (RMSE), and Mean Absolute Error (MAE) error measures. According to the prediction results of MAPE, RMSE, and MAE values of ANN, VMD-ANN, GRU-ANN, and JAYA-ANN hybrid models in summer and spring seasons, the JAYA-ANN hybrid model is better than other prediction models and provides higher forecasting accuracy. Such a forecasting model can be an important guide for energy planners and local electricity providers for generation planning and management of alternative energy sources.

Keywords Artificial neural network, wind energy, hybrid learning, forecasting.

1. Introduction

The world energy deficit and environmental pollution have become increasingly severe. Many developing countries are increasingly opting for renewable energy sources in electricity generation. This method not only allows individuals to meet their own household energy needs but also enables them to sell any surplus electricity they generate to connected energy providers [1]. Wind energy has been recognised as a cleaner and renewable energy source and has been included in the country's national long-term energy promotion strategy. According to the Global Wind Energy Council, the total installed wind power capacity of the world has reached 1 TW according to the 2024 report [2]. However, the intermittent and variable nature of wind power raises a number of problems, included those related to the stability of wind power supplies and the sensitive balance between the management and capacity in reserve [3]. Thus, forecasting of reliable wind power is essential for the security of the power grid and for pre-determining the power strategy [4], [5].

Cite this article as: B. Tasdemir and M. Yaz, "Comparative Short-Term Wind Energy Forecasting Using Hybrid JAYA-ANN, GRU-ANN, and VMD-ANN Models" *International Journal of Smart Grid (ijSmartGrid)*, Vol. 10, No. 1, pp. 14-29, March, 2026.

Existing methods for wind energy prediction mainly consist of statistical modelling and physical models [6]. Physical methods rely on advanced mathematical models to make predictions. These methods utilize numerical weather forecast data provided by meteorological services, which analyze the behavior and physical dynamics of the lower atmosphere to forecast future weather conditions. Additionally, they take into account the topography of the wind farm's location. However, a major drawback of physical models is their dependence on highly precise online and offline data [7]. They are also computationally intensive and demand substantial resources [8]. Physical methods excel in medium- and long-term forecasting, but their accuracy diminishes for short-term predictions. In contrast, statistical methods focus on identifying linear and non-linear relationships between weather variables such as wind speed, direction, temperature and the wind power generated [9]. These methods rely on historical data to train models that establish these connections. While statistical models are well-suited for short-term wind forecasting, their accuracy decreases as the forecasting horizon extends. They are relatively simple to implement and involve minimal computation time. To enhance performance, these models are periodically updated by comparing predicted and actual power values, allowing forecasts to improve over time.

Physical, statistical, and machine learning-based methods have made significant advances in wind energy forecasting and various other disciplines, demonstrating the diversity and potential of the field. Environmental studies integrating machine and deep learning techniques, in particular, have achieved high accuracy [10].

This study systematically analyzes selected works published between 2021 and 2023, focusing on estimation time, data set size, model structures, and evaluation criteria, as summarized in Table 1. The comprehensive literature review indicates that, despite notable progress, several fundamental challenges remain unresolved.

In this study, meteorological and wind farm data commonly utilized in daily wind power forecasting are employed. Initially, an ANN based forecasting model is developed and evaluated using wind direction, PM10 concentration, temperature, and historical power output data. Subsequently, three hybrid models JAYA-ANN, GRU-ANN, and VMD-ANN are constructed using the same dataset and compared against the standalone ANN model. The results indicate that the hybrid models exhibit superior forecasting performance. This study provides a meaningful contribution to the academic literature on short-term wind energy forecasting. Furthermore, the integration of the JAYA-ANN hybrid model and the inclusion of the PM10 parameter both of which have not been previously applied in wind energy forecasting constitute a significant innovation introduced by this research.

2. Methodology

In this section ANN, JAYA, GRU, and VMD algorithms used in the construction of hybrid forecasting models are presented in detail. The overall training architecture is illustrated in Figure 1. In the proposed approach, the JAYA, GRU, and VMD algorithms are employed to optimize the internal parameters of the ANN, namely the weights and biases of the multilayer perceptron. These optimization algorithms receive the ANN parameters as input vectors and iteratively adjust them to minimize forecasting error. The objective function guiding this optimization process is based on widely used error metrics, including RMSE, MAE, and MAPE.

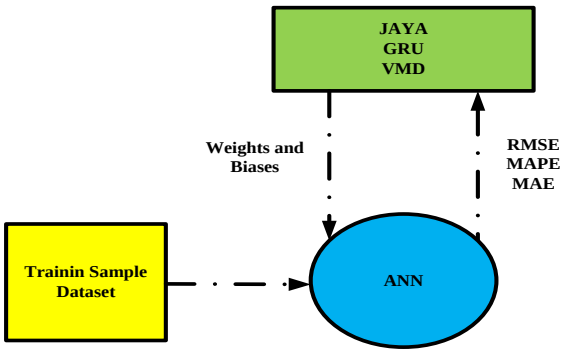

Fig. 1. Architecture of training examples.

2.1. Artificial Neural Networks

Artificial Neural Networks are non-linear mapping systems designed to emulate the workings of the human central nervous system. At their core lies the basic building block: the neuron. The first ANN model, introduced by McCulloch and Pitts in 1943, laid the foundation for concepts that remain relevant today [18]. ANNs can also be characterized as highly parallel processors made up of simple processing units capable of learning from experience and applying this knowledge to make future decisions [19]. ANNs are robust prediction tools for situations where the relationship between data is unknown and needs to be established. They learn from any observed patterns in the relationships between input datasets and target values in the training dataset. Once an ANN is trained, it can predict future outcomes based on the identified patterns and connections derived from the training dataset.

ANNs are particularly well-suited for processing data that are uncertain, noisy, or exhibit occasional irregular variations, making them highly effective for modeling complex real-world phenomena. Consequently, ANNs are ideal for forecasting both wind speed and wind power, as they can capture complex, non-linear dependencies that traditional linear models may fail to represent accurately [18].

Their highly interconnected nodes allow neural networks to learn intricate patterns from the training data and generalize these patterns to unseen data in a manner that loosely resembles the adaptive and learning processes of the human brain. This capacity for learning, adaptation, and generalization represents one of the principal advantages of ANNs, particularly in forecasting applications where input-output relationships are dynamic, stochastic, and potentially noisy. Figure 2 illustrates the fundamental architecture of an artificial neural cell, highlighting the interconnections and the flow of information through the network.

Table 1. Lists illustrative research on wind energy power forecasting from 2021 to 2023

Year	Ref.	Period	Dataset length	Forecast model	Forecast error	Comments
2023	S. M. Malakouti [11]	1 h	One and a half months	Random Forest Ada Boost K - Neighbors	MSE=21-2340.8-32286.9 kW RMSE=4.6-48.38-179.68 kW MAE=2.56-38.09-116.62 kW MAPE=0.0079-2.78-16.33 % R^2=1-0.997-0.95	Random Forest demonstrated superior predictive performance, whereas KNN exhibited lower accuracy despite faster computation.
2023	Gao et al. [12]	15 minutes	3000 sample points	SSA-VMD-LSTM	MAE=1.4139 RMSE=2.0296 MAPE=0.0849 %	The results show that the SSA-VMD-LSTM method gives better prediction accuracy and lower wind power error than other methods, proving the model is effective.
2023	Alkabbani et al. [13]	1 h	3 years	MIMO ANN MIMO LSTM	R^2=0.77-0.77 MSE=1.83-1.68 RMSE=427.78-409.88 MW MAPE=27.5-26.6 %	Multi-input multi-output (MIMO) LSTM approach are more reliable with higher accuracies.
2022	Xiong et al. [14]	1 h/ 2h 3 h	1 years	AMC-LSTM	MAE=0.0509-0.0517-0.0519 RMSE=0.0949-0.0954-0.0948 MSE=0.8951-0.9112-0.8990	The proposed wind power forecasting model has lower error, higher accuracy, and better matches the actual data compared to other models.
2022	Zhu et al. [15]	1 h	6 month	CEEMDAN-SVR-TCN	MAE=68.4695-75.7741-75.21 RMSE=87.9475-98.9572-100 MSE=3.3726-3.7948-3.835	Using real wind power data, the proposed method shows better accuracy than other models, proving its effectiveness.
2022	He et al. [16]	15 minutes	16 month	IOWA-CNN-LSTM	RMSE=12.154 MAE=8.0608	The proposed model has the lowest MAE and RMSE among the five models, showing it is reliable and effective.
2021	Chandran et al. [17]	10 minutes	50.530 data	LSTM GRU RNN	MSE=0.1358-0.13-0.143	The GRU network is particularly well-equipped to capture highly non-linear and complex patterns in real-time data.

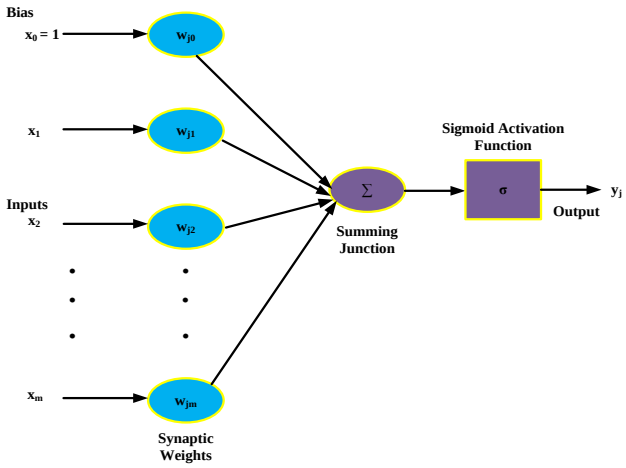

Fig. 2. Artificial neural cell architecture.

Where:

- X_1 and x_m represent the inputs of the neuron.
- X_0 represents the bias. The bias helps neurons activate meaningfully. It determines the threshold at which a neuron activates; otherwise, the neuron remains inactive.
- W_{j0} and w_{jm} represent the respective synaptic weights connecting each input to neuron j.
- Y_j is the output signal of the neuron.

The output of the summation function is shown as (s_j) in equation 1:

$$s_j = \sum_{m=0}^{m} w_{jm} x_m \quad (1)$$

The sum of the weights is then passed through an activation function (σ) to compress it into a specific small value range. In Equation 2, the output obtained from the activation function is the output of the neuron (y_j).

$$y_j = \sum_{m=0}^{m} \sigma(s_j) \quad (2)$$

In this study, an ANN model with 4 input layers, one hidden layer, and one output layer is used for daily wind energy power forecasting. In the structure of ANN, a single hidden layer with 5 neurons and a sigmoid activation function is used because it is easy to calculate the derivative by compressing the inputs between 0 and 1 [20]. The trial-and-error method was adopted to determine the number of neurons in the hidden layer. As a result of the experiments, the best network topologies for each product series are shown in Table 2.

Table 2. Performance of the developed ANN model

Model Used	Fuction	Neuron Count	MAPE (%)	RMSE (MW)	MAE (MW)
ANN	Sigmoid	5	19.59	22.63	1.28
ANN	Sigmoid	10	20.71	24.46	1.78
ANN	Sigmoid	15	23.25	26.19	2.15
ANN	Sigmoid	20	25.89	28.28	2.45

Artificial neural networks are classified into feedforward networks and feedback networks based on their structures.

2.2. Feedforward Neural Networks

In feedforward artificial neural networks, processing elements are typically organized in layers. Signals are transmitted in a unidirectional manner from the input layer to the output layer through connections. In a feedforward ANN, cells are arranged in layers, and the outputs of the cells in each layer are transferred as inputs to the next layer with weights. The input layer sends information received from the external environment directly to the cells in the hidden layer without any modifications. The information is processed in the hidden and output layers to obtain the network's result output [21]. Figure 3 shows the feed-forward network structure.values in the training dataset. X_s represent inputs, and Y_s represent outputs.

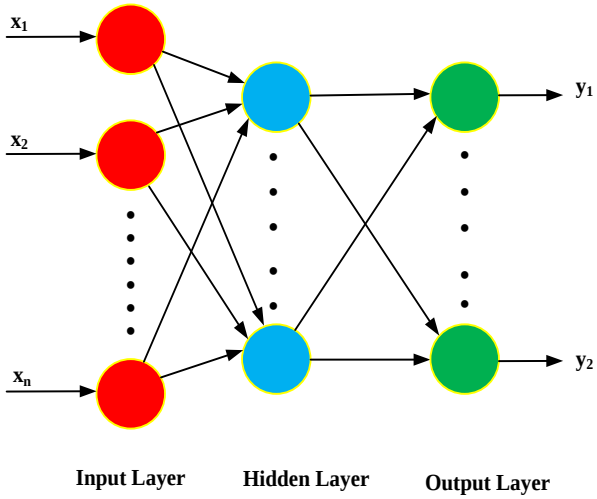

Fig. 3. Feedforward network structure.

In this study, we chose ANN as our base model because it is lightweight, widely used in the literature, and suitable for the size of our dataset. This allows us to clearly evaluate the contribution of our proposed method independently of the effects of complex deep architectures. The feedforward neural network structure is preferred to solve problems due to its prediction ability and its success in tasks such as pattern recognition, visual recognition, and time series prediction.

2.3. Feedback Neural Networks

Recurrent or feedback artificial neural networks have a variable structure, unlike feedforward networks. In these networks, neurons in the output or intermediate layers send their outputs back to the input layer or previous intermediate layers. Thus, information is transmitted both forward and backward. Feedback neural networks have dynamic memory, where the output at any given time is a reflection of both the current and previous inputs. In feedback neural networks, the output of at least one processing element is fed back either to itself or to other elements, and this feedback is typically provided through a delay element. Feedback occurs not only between processing elements but also between layers. Due to

this structure, feedback neural networks exhibit nonlinear dynamic behaviors. As a result, depending on how the feedback is implemented, these networks can appear in different structures and behaviors [22]. Figure 4 shows the feedback neural network structure.

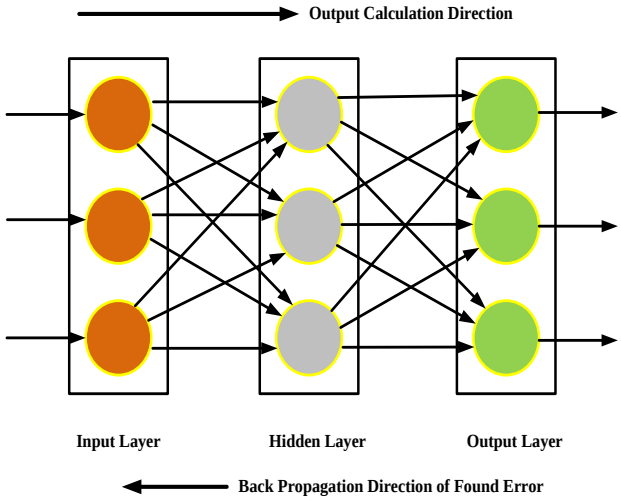

Fig. 4. Feedback network structure.

2.4. Jaya Algorithm

The basic Jaya algorithm, while having many advantages in solving various optimization problems, also has some disadvantages, such as low accuracy and slow convergence, particularly for complex and high-dimensional problems, due to the challenges in balancing the search and development processes. In recent years, many researchers have made various improvements to address these shortcomings of the Jaya algorithm and have successfully applied the algorithm to different practical problems.

In The Jaya algorithm is a population-based metaheuristic method introduced by Rao and used for solving constrained and unconstrained continuous optimization problems. Being independent of parameters is one of the most important features that distinguish the Jaya algorithm from others. Thanks to this advantage, it can be easily adapted to optimization problems. In addition, one of the strengths of the algorithm is that it increases the tendency to move towards the best solution during location updates, while at the same time avoiding the worst solution and reducing the risk of getting stuck in the local maximum or minimum [23]. Due to these advantages, JAYA algorithm is preferred in this study.

Assume that the objective function is Z(x) to be maximized or minimized and that at any iteration 'i', 'k' is the number of design variables and 'n' is the population size. Let the best and worst values of the objective function during an iteration be denoted by $Z_{k,best,i}$ and $Z_{k,worst,i}$ respectively. Also, $X_{k,best,i}$ and $X_{k,worst,i}$ are the best and worst values of variable 'k' during iteration 'i' corresponding to $Z_{k,best,i}$ and $Z_{k,worst,i}$ in the population, respectively. The updated value is then calculated according to equation 3.

$$x'_{k,n,i} = x_{k,n,i} + r_{1,k,i}(x_{k,best,i} - |x_{k,n,i}|) - r_{2,k,i}(x_{k,worst,i} - |x_{k,n,i}|) \quad (3)$$

Here $r_{1,k,i}$ and $r_{2,k,i}$ are two random numbers between [0,1]. The term '$r_{1,k,i}$ ($X_{k,best,i}$ - $|x_{k,n,i}|$)' indicates the ability of the solution to approach the best solution, while the term '$r_{2,k,i}$ ($X_{k,worst,i}$ - $|x_{k,n,i}|$)' indicates the ability of the solution to avoid the worst solution. $X_{k,n,i}$ is accepted if it gives a superior function value. Two random numbers, $r_{1,k,i}$ and $r_{2,k,i}$ are used for the Jaya algorithm to enable better exploration of the search space. The absolute value $|x_{k,n,i}|$ used in the equation helps the algorithm to further increase its exploration ability. The JAYA algorithm used in this study was run 30 times in 1000 iterations, and the number of populations was taken as 50, which is the algorithm run parameter. Figure 5 shows the flow diagram of the JAYA algorithm.

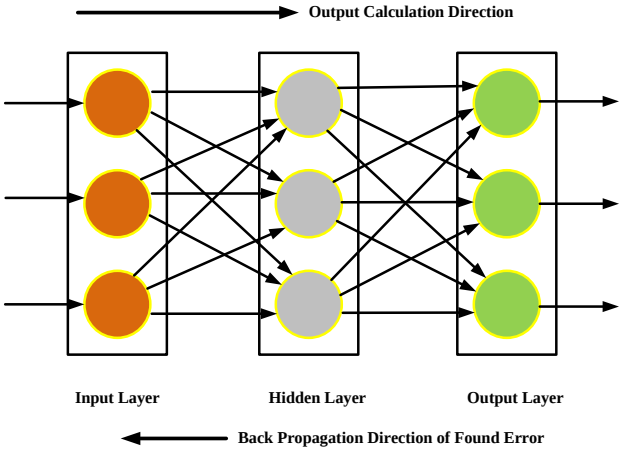

Fig. 5. Flow diagram of the JAYA algorithm.

2.5. Gated Recurrent Unit (GRU)

GRU, first proposed by Cho et al. in 2014, is a gated recurrent neural networks (RNN) derivative developed to address the inadequacies of traditional RNN in learning long-term dependencies [24]. GRU uses an update gate and a reset gate to provide a more stable learning process, especially against problems such as gradient fading and bursting, which are frequently encountered in RNNs.

Compared to the LSTM architecture, the GRU appears to have a structurally simpler design. The LSTM consists of three gates: the input gate, the forget gate, and the output gate; it also contains an additional memory unit called the cell state. GRU combines these mechanisms into two gates, integrating the cell state and the hidden state into a single structure. This simplification reduces the number of parameters and reduces the computational cost [25]. The lower computational complexity of GRU allows it to offer faster training times compared to LSTM in some applications while achieving similar accuracy levels without significant loss in performance. For this reason, GRU has become a preferred alternative, especially in systems with limited resources or online applications [26].

The GRU-based neural network architecture developed in this study is presented in detail in Figure 6. The model consists of five main components: the input layer, the GRU layer, the dropout layer, the fully connected layer, and the output layer. The GRU layer, which is at the center of this structure, acts as

the basic computational unit of the network and has the ability to learn both short-term and long-term dependencies in time series data. The GRU layer converts the data it receives from the input into temporal representation vectors, enabling their use in the subsequent layers of the network. The dropout layer, placed immediately after the GRU layer, randomly disables certain neurons during the training process, preventing the model from overfitting to certain features. This mechanism reduces overfitting by preventing reliance on specific connections. As a result, the model achieves more balanced learning and its generalization ability increases when faced with different data samples, thus making prediction performance more reliable [27]. Furthermore, the dropout layer increases the model's flexibility against different data samples, strengthening its robustness against noisy or missing data.

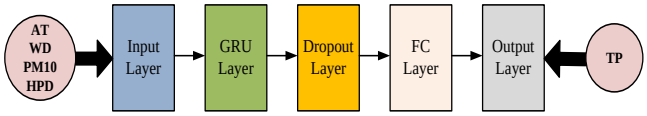

Fig. 6. Architecture of the GRU network.

As shown in Figure 7, the relevant GRU layer consists of multiple GRU blocks, and this figure also presents the schematic structure of a single GRU block. Two main control mechanisms, the reset gate and the update gate, form the basis of this architecture. The reset gate allows the network to model short-term dependencies more efficiently by determining the extent to which past memory is integrated with new input information. On the other hand, the update gate offers selective control over the extent to which the previous hidden state is maintained or updated.

As indicated in the diagram, the inputs to the GRU block are defined as the input vector X_t at the current time step and the hidden state H_{t-1} from the previous time step. As a result of the computations, a candidate latent state $\hat{H}$ is generated, and this information is updated to the final latent state H_t through the update mechanism. This process enables GRU to learn the context in temporal data more efficiently. The mathematical calculation formulas in Equations 4, 5, 6, and 7 form the quantitative basis of this process.

$$R_t = \sigma(X_t W_{xr} + H_{t-1} W_{hr} + b_r) \quad (4)$$

$$Z_t = \sigma(X_t W_{xz} + H_{t-1} W_{hz} + b_z) \quad (5)$$

$$\hat{H}_t = \tanh(X_t W_{xh} + (R_t \odot H_{t-1}) W_{hh} + b_h) \quad (6)$$

$$H_t = Z_t \odot H_{t-1} + (1 - Z_t) \odot \hat{H}_t \quad (7)$$

R_t and Z_t represent the reset gate and update gate, respectively; σ and tanh denote the sigmoid activation function and hyperbolic tangent activation function, respectively; ʘ denotes the element-wise multiplication operation. W_{xr}, W_{xz}, W_{hr}, W_{hz}, W_{xh}, and W_{hh} are the weight parameter matrices associated with the input and hidden states, while b_r, b_z, and b_h are the corresponding bias vectors. These parameters are learned during the training process and play a crucial role in regulating the flow of information within the gated recurrent unit structure, enabling the model to effectively capture temporal dependencies and nonlinear patterns in sequential data.

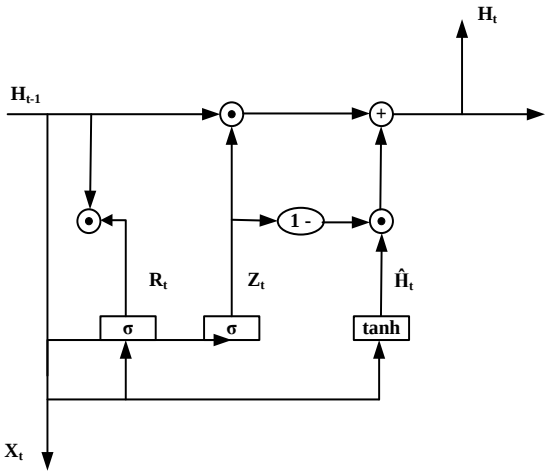

Fig. 7. Diagram of GRU block.

2.6. Variational Mode Decomposition (VMD)

Variational Mode Decomposition (VMD), developed by Dragomiretsky et al. in 2014, is a non-iterative and adaptive signal processing method formulated in a variational framework to decompose signals into predefined modes [28]. Compared to Empirical Mode Decomposition (EMD) and similar empirical approaches, VMD offers higher adaptability to signals with varying frequency content [29], superior decomposition accuracy [30], and a bandwidth-oriented control mechanism by optimizing the center frequency of each mode. Thanks to these features, VMD is often preferred in the preprocessing stage to provide reliable and meaningful feature extraction for machine learning-based models. It has been shown that VMD can decompose non-stationary signals into more discrete and information-rich components in the time-frequency plane [31]. In this context, VMD-based decomposition stands out as an effective tool to improve the performance of learning tasks such as noise suppression, pattern recognition, and classification.

$$\min\left\{\sum_{k=1}^{k} \left\| \partial_t[(\delta(t) + \frac{j}{\pi t}) u_k(t)] \exp(-j w_k t \right\|\right\}$$

$$\{u_k, w_k\} \quad (8)$$

$$s.t. \sum_{k=1}^{N} u_k = f(t)$$

In Equation 8, 'u_k' denotes the kth modal component representing each sub-signal obtained by decomposition, 'w_k' signifies the center frequency of the kth power modal component, 'j' is the imaginary unit, 'N' denotes the number of modal decompositions, 'δ(t)' is the Dirac function, i.e., the unit impulse function, '∂_t' is the derivative, and 'f(t)' is the original signal to be decomposed. The VMD based decomposition process is carried out in the following specific steps.

Step 1: Initialise $\{u_k^1\}$, $\{w_k^1\}$, λ_k^1 and n =0;

Step 2: n=n+1, enter the loop;

Step 3: The update formulas for u_k and w_k are applied iteratively until the number of parses reaches N, at which point the inner loop ends

Step 4: The value of λ is updated via an update formula at each iteration.

Step 5: Given a tolerance ϵ, the loop is terminated if the stopping condition (9) is fulfilled. In the equation, ε represents the convergence progression.

$$\sum k\|u_k^{n+1} - u_k^n\|_2^2 / \|u_k^n\|_2^2 < \epsilon \quad (9)$$

Otherwise, the loop continues with Step 2.

2.7. Persistence Reference Model (PRM)

The persistence forecasting model is a fundamental reference approach frequently employed in time series forecasting applications. Its primary advantages lie in its ease of implementation and very low computational cost. The key objective in developing more advanced forecasting models is to achieve higher forecasting accuracy than the persistence model, ideally while maintaining a similar or lower computational burden. This model operates on the assumption that the wind power output at time t+1 is highly correlated with the output at time t. Accordingly, the future wind power output is directly estimated as a continuation of the current output. This approach can demonstrate notable forecasting performance, particularly in scenarios where short-term fluctuations in wind generation are minimal.

The persistence model is commonly employed as a benchmark for evaluating the performance of various forecasting methods. However, its forecast accuracy is significantly influenced by the length of the forecast horizon; as the horizon extends, the model's accuracy tends to decline. Furthermore, variations in meteorological parameters such as temperature, solar radiation, wind speed, and humidity can considerably affect its performance. Owing to these limitations, persistence-based forecasting models typically yield higher prediction errors and are therefore widely used as baseline models for assessing the accuracy of more advanced forecasting approaches. In the study by Perez et al. [32], a comparable methodology was applied, wherein the performance of the proposed forecasting model was evaluated against the results obtained from the persistence model. The percentage improvement is defined in Equation 10. In this equation, e_{TM} is the prediction model error, e_{SRM} is the continuous reference model error, and p_{IY} is the improvement percentage. progression.

$$P_{IY} = \left(1 - \frac{e_{TM}}{e_{SRM}}\right) x100 \quad (10)$$

3. Results

The dataset was obtained from an onshore wind farm in Turkey's Central Anatolia region. This climate differs from coastal or tropical wind farms in terms of boundary layer behavior, low humidity, and stable wind regime. Therefore, direct generalization of the model is not recommended. Which comprises three different wind turbines whose specifications are summarized in Table 3. The dataset presented in Table 4 includes wind direction, PM10, and temperature measurements for the year 2022, while the corresponding output power data from 2021 is used on a daily basis. The study is based on the transfer forecasting approach in wind energy prediction. The aim is not to directly copy power values but to learn the meteorological variable production relationship and apply it to the following year's atmospheric data. This method is common in the energy sector, prevents the machine from overfitting, and generalizes the physical behavior of the local wind regime. The dataset collected during the spring and summer periods contains no missing values. During the winter season, atmospheric conditions are more irregular: factors such as condensation, freezing, low temperatures, high turbulence intensity, and sudden wind shear breaks increase the model's variance, making comparisons methodologically difficult. This study first aims to demonstrate the relative strength of hybrid models during periods of high seasonal stability. Of the entire dataset, 80% was used for training, 10% for validation, and the remaining 10% for testing.

The dataset collected during the spring and summer periods contains no missing values. Of the entire dataset, 80% was used for training, 10% for validation, and the remaining 10% for testing.

Table 3. Information on three different wind turbines in the wind farm

Wind Turbine	**E82-E2**	**E82-E3**	**E82-E5**
Nominal power (kW)	2000	3000	2350
Rotor diameter (m)	80	82	82
Navel height (m)	78	78	78
Wind length (m)	38.8	38.8	43.8

Table 4. Data set

Input	**Output**
Wind direction	Output power
PM10	
Temperature	
Historical output power	

In our study, the PM10 parameter is treated not merely as an additional meteorological input, but as a physical atmospheric variable that influences the aerodynamic behavior of wind flow. High particle concentration reduces momentum transfer on the rotor surface, decreasing the efficiency of the effective power curve and introducing systematic deviations in the wind speed–power relationship. When PM10 was included in the model, an improvement of 10–15% was observed in MAPE values. This result confirms the variable's contribution to prediction performance. A computer with an Intel Core i5-1135G7 CPU @ 2.40 GHz and

16 GB of RAM was used to implement the study with Matlab. Table 5 shows the computational costs of hybrid models.

Table 5. Computational costs of hybrid models

Model	Average education time	Explanation
ANN	3-4 min	Lower cost
VMD-ANN	6-7 min	VMD analysis
GRU-ANN	10-12 min	Time dependent account
JAYA-ANN	14-16 min	Global optimization 1000 iterations x50 populations

Although JAYA-ANN has the highest computational cost, it offers an improvement in prediction error in the range of 60–75%. Therefore, the method is technically rational.

Since wind power is a highly variable parameter, wind power forecasting is not an exact science. The error rate is calculated by comparing the predicted wind power at a certain time 't' with the actual power value in the data set. A low error indicates the accuracy of the prediction model. The evaluation criteria to be used in this study are root mean square error and mean absolute percentage error. The RMSE, MAPE, and MAE error evaluation formulas are provided in Equations 11, 12, and 13, respectively [33].

$$RMSE = \sqrt{\frac{1}{n}\sum_{i=1}^{n}\left(X_{est,i} - X_{tar,i}\right)^2} \quad (11)$$

$$MAPE = \frac{100}{n}\sum_{i=1}^{n}\left|\frac{X_{est,i} - X_{tar,i}}{X_{tar,i}}\right| \quad (12)$$

$$MAE = \frac{1}{n}\sum_{i=1}^{n}\left|X_{est,i} - X_{tar,i}\right| \quad (13)$$

Where:

- $X_{est,i}$= forecast value for time i
- $X_{tar,i}$ = actual value observed at time I
- i = number of forecast points

3.1. Forecast Results for the Summer Period

In the prediction using the ANN model, the MAPE values for the training, validation, and test subsets of the dataset were found to be 19.92%, 18.69%, and 17.81%, respectively. The corresponding RMSE values were calculated as 26.22 MW, 50.84 MW, and 66.78 MW, while the MAE values were 2.13 MW, 13.14 MW, and 15.97 MW, respectively. Figure 8 presents the prediction results for the training, validation, and test subsets of the dataset.

In the prediction using the VMD-ANN hybrid model, the MAPE values for the training, validation, and test subsets of the dataset were found to be 17.54%, 15.93%, and 14.02%, respectively. The corresponding RMSE values were calculated as 24.39 MW, 41.75 MW, and 38.06 MW, while the MAE values were 2.12 MW, 18.45 MW, and 10.98 MW, respectively. Figure 9 illustrates the prediction performance of the model across all subsets.

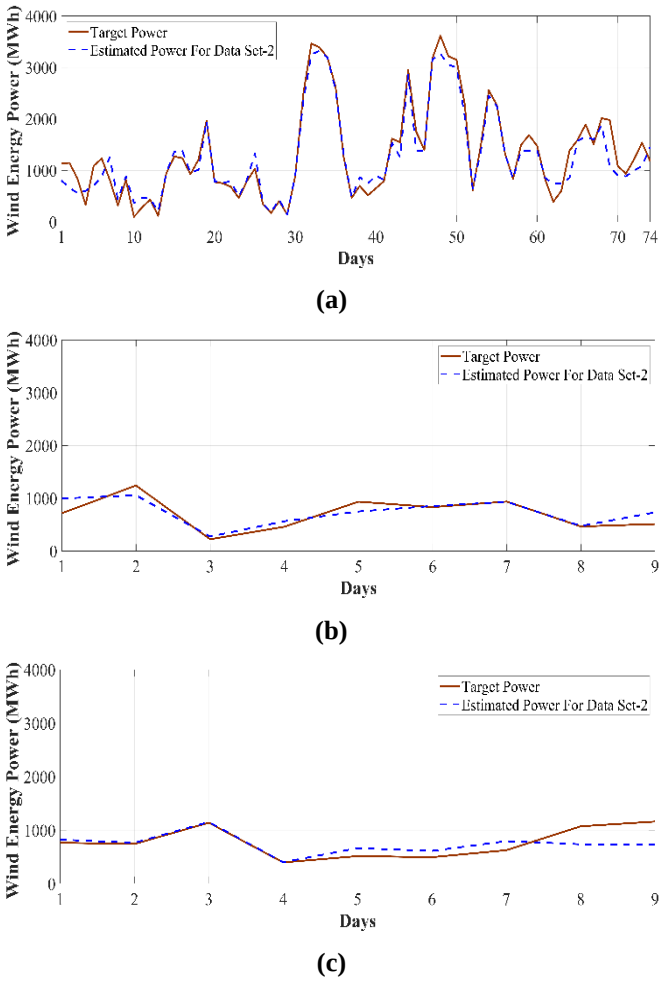

Fig. 8. Prediction results for the ANN model based on three subsets of the dataset: (a) training subset, (b) validation subset, and (c) testing subset.

The forecasting performance of the GRU-ANN hybrid model was evaluated based on the training, validation, and test subsets of the dataset. MAPE values were found to be 14.45% for the training set, 13.33% for the validation set, and 11.76% for the test set, indicating a consistent improvement in generalization capability. In parallel, RMSE values were computed as 23.10 MW, 35.73 MW, and 37.70 MW, while MAE values were 1.68 MW, 12.31 MW, and 10.21 MW, respectively. Figure 10 provides a graphical representation of the prediction performance across all subsets.

To assess the predictive capability of the JAYA-ANN hybrid model, performance metrics were examined for the training, validation, and test subsets of the dataset. MAPE was measured at 9.49% for the training data, 8.35% for the validation data, and 7.28% for the test data, reflecting the model's improved generalization on unseen data. Additionally, RMSE values were determined to be 14.56 MW, 31.75 MW, and 23.80 MW, while the corresponding MAE values were calculated as 0.99 MW, 7.55 MW, and 5.93 MW for the respective subsets. The model's prediction accuracy across all subsets is visually depicted in Figure 11. These results indicate that the proposed JAYA-ANN model demonstrates a reliable and robust performance in short-term wind power forecasting.

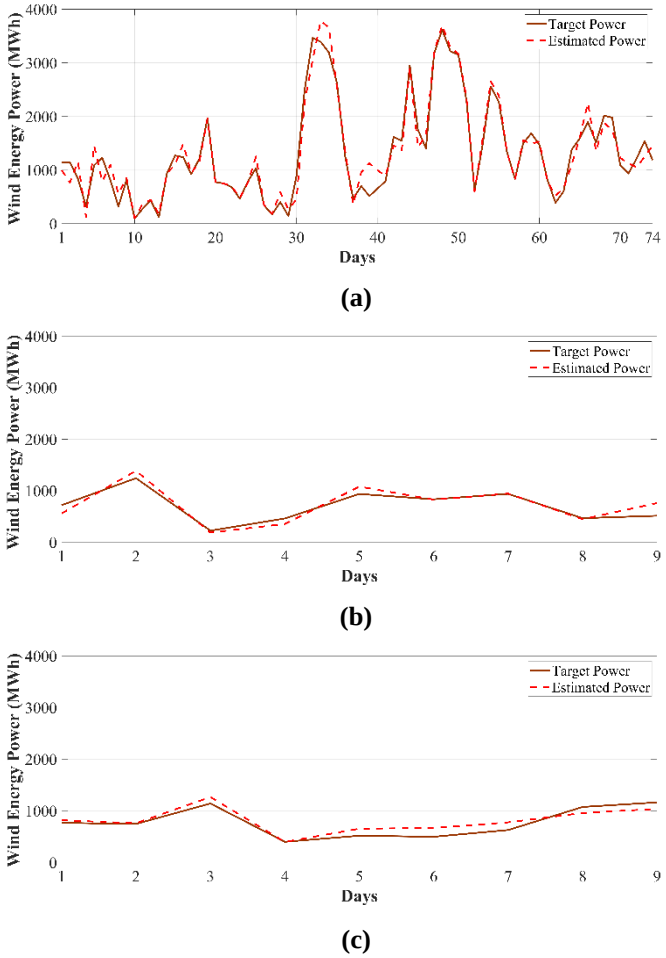

Fig. 9. Prediction results for the VMD-ANN model based on three subsets of the dataset: (a) training subset, (b) validation subset, and (c) testing subset.

The predictive performance of the ANN, VMD-ANN, GRU-ANN, and JAYA-ANN hybrid models was assessed through a comparative analysis of key evaluation metrics. Specifically, MAPE values were 19.59%, 17.04%, 14.08%, and 8.36%, respectively. In terms of RMSE, the models yielded values of 33.85 MW, 27.29 MW, 25.53 MW, and 17.14 MW. The corresponding MAE values were calculated as 4.91 MW, 4.16 MW, 3.15 MW, and 1.88 MW. These results clearly indicate that the JAYA-ANN model outperformed the others in terms of overall prediction accuracy. A visual comparison of the model performances is provided in Figure 12.

The proposed prediction models are generally not directly comparable to models in other studies, as each is based on different datasets with their own unique characteristics. The literature indicates that different datasets can affect a model's learning capacity and prediction accuracy; therefore, model performance should be evaluated relative to a standard reference model. To this end, the continuity model error is used to measure model performance more reliably. The continuity model error is based on the principle of making future predictions using values observed in the previous time step, thereby establishing a reference prediction standard. This error can be derived using Equations (6), (7), and (8). The predicted values are obtained by shifting the actual observed data by one time step and serve as a reference reflecting the model's baseline performance level.

Table 6 comprehensively and thoroughly presents the prediction performance of the four different modeling approaches considered in this study, namely the independent ANN, hybrid VMD-ANN, GRU-ANN, and JAYA-ANN models. The table enables a rigorous comparison in terms of prediction accuracy and overall effectiveness by evaluating the performance of each model on the same dataset. This clearly highlights the strengths and weaknesses of each model in the context of the dataset and provides important information to consider when selecting a model.

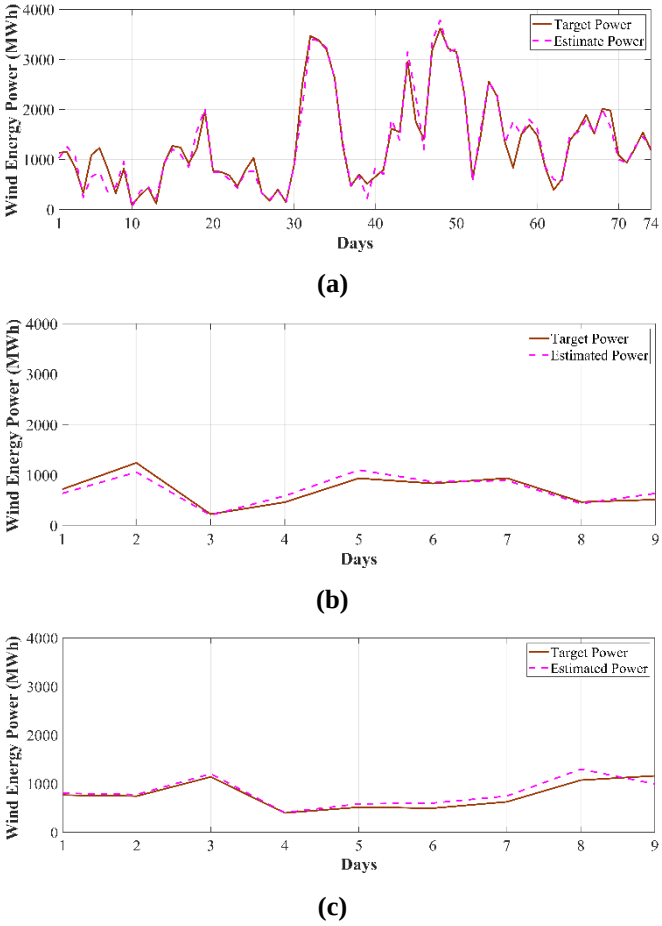

Fig. 10. Prediction results for the GRU-ANN model based on three subsets of the dataset: (a) training subset, (b) validation subset, and (c) testing subset.

3.2. Forecast Results for the Spring Semester

The ANN prediction model was evaluated using spring season data by comparing key performance metrics across different model configurations. MAPE values were recorded as 20.45%, 19.81%, and 16.53%, respectively; this demonstrates varying levels of relative prediction accuracy and highlights improvements achieved with more advanced modeling approaches. Regarding RMSE, the models produced values of 26.38 MW, 47.22 MW, and 40.2 MW. The corresponding MAE values were recorded as 1.71 MW, 11.9 MW, and 8.76 MW, further clarifying the average prediction errors and each model's effectiveness in capturing actual wind

power variations. Figure 13 graphically displays the comparative prediction performance of the models and allows for a clear visual assessment of the relative strengths and weaknesses of the models across the evaluation criteria.

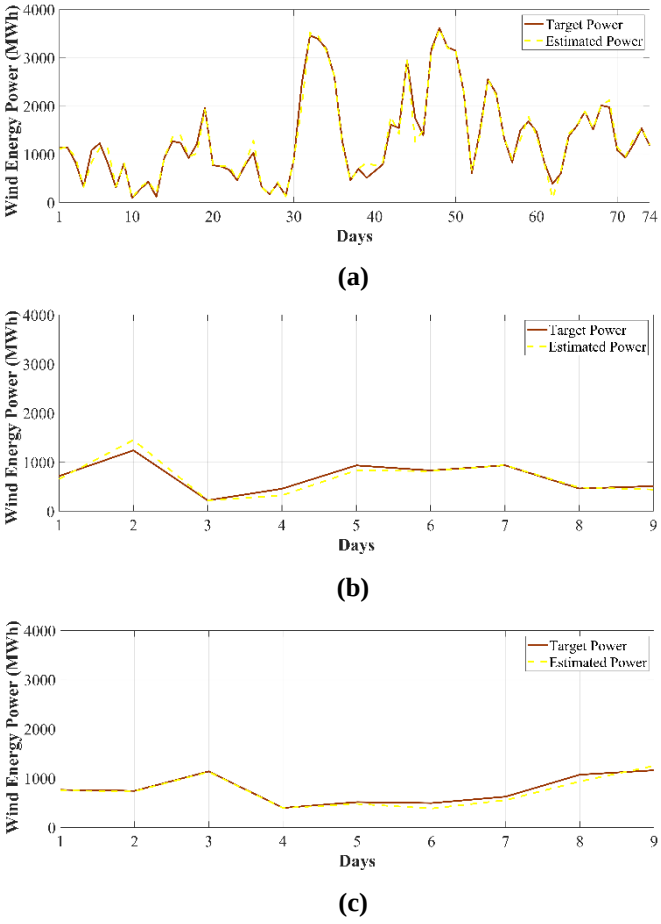

Fig. 11. Prediction results for the JAYA-ANN model based on three subsets of the dataset: (a) training subset, (b) validation subset, and (c) testing subset.

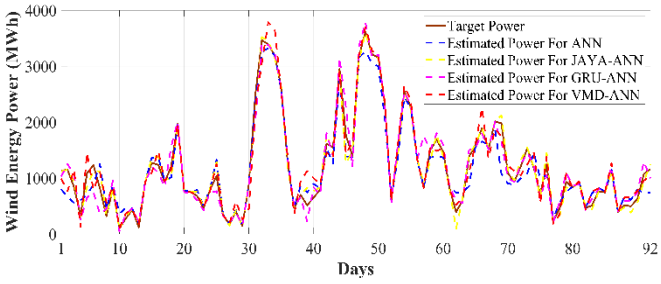

Fig. 12. Prediction results for ANN, VMD-ANN, GRU-ANN, and JAYA-ANN models.

The predictive performance of the VMD-ANN model was analyzed using data from the spring season through a comparative assessment of key evaluation metrics. MAPE values were observed to be 18.39%, 17.71%, and 17.02%, respectively. In terms of RMSE, the model yielded values of 15.54 MW, 27.74 MW, and 18.35 MW. The associated MAE values were calculated as 1.39 MW, 8.47 MW, and 4.71 MW. A visual comparison of these forecasting results is illustrated in Figure 14.

Table 6. MAPE, RMSE, and MEA values according to summer forecast results

Models	MAPE (%)	RMSE (MW)	MAE (MW)
ANN (training)	19.92	26.22	2.13
VMD-ANN (training)	17.54	24.39	2.12
GRU-ANN (training)	14.45	23.10	1.68
JAYA-ANN (training)	9.49	14.56	0.99
ANN (validation)	18.69	50.84	13.14
VMD-ANN (validation)	15.93	41.75	18.45
GRU-ANN (validation)	13.33	35.73	12.31
JAYA-ANN (validation)	8.35	31.75	7.55
ANN (test)	17.81	66.78	15.97
VMD-ANN (test)	14.02	38.06	10.98
GRU-ANN (test)	11.76	37.70	10.21
JAYA-ANN (test)	7.28	23.80	5.93
ANN (all)	19.59	33.85	4.91
VMD-ANN (all)	17.04	27.29	4.16
GRU-ANN (all)	14.08	25.53	3.15
JAYA-ANN (all)	8.36	17.14	1.88
PRM	33.25	66.99	11.96

The forecasting performance of the GRU-ANN model was thoroughly evaluated using several key performance metrics to assess its accuracy and reliability in predicting wind power outputs. The MAPE values were recorded as 15.81%, 14.26%, and 13.02%, respectively, indicating a notable improvement in relative prediction accuracy compared to baseline models and highlighting the model's ability to effectively capture the non-linear characteristics of the data. In terms of RMSE, the model yielded values of 14.27 MW, 29.4 MW, and 16.36 MW, reflecting the magnitude of absolute deviations from the observed measurements and providing insight into the overall predictive precision of the model. Meanwhile, the MAE was calculated as 1.25 MW, 8.18 MW, and 4.38 MW, further illustrating the average errors and demonstrating the model's capability to produce consistently reliable forecasts. A graphical comparison of these prediction outcomes is presented in Figure 15, offering a clear visual representation of the GRU-ANN model's performance across different evaluation criteria and enabling an intuitive assessment of its strengths relative to other forecasting approaches.

The forecasting performance of the JAYA-ANN model was comprehensively assessed using several key evaluation metrics to determine its accuracy and reliability in predicting wind power generation. The MAPE values were recorded as 12.76%, 12.45%, and 11.33%, respectively, demonstrating a consistently high relative prediction accuracy and indicating

the model's capability to effectively capture the non-linear and fluctuating nature of wind power data. The corresponding RMSE values were found to be 13.94 MW, 21.95 MW, and 19.93 MW, reflecting the magnitude of absolute deviations between the predicted and observed values and providing insight into the overall precision of the model. Furthermore, the MAE was determined to be 1.03 MW, 6.01 MW, and 4.12 MW, highlighting the average prediction errors and confirming the model's robustness in producing reliable forecasts across different time steps. Figure 16 presents a visual representation of these prediction outcomes, allowing for an intuitive comparison of the JAYA-ANN model's forecasting performance with other models and facilitating a clear understanding of its strengths and limitations in capturing the dynamics of wind power generation.

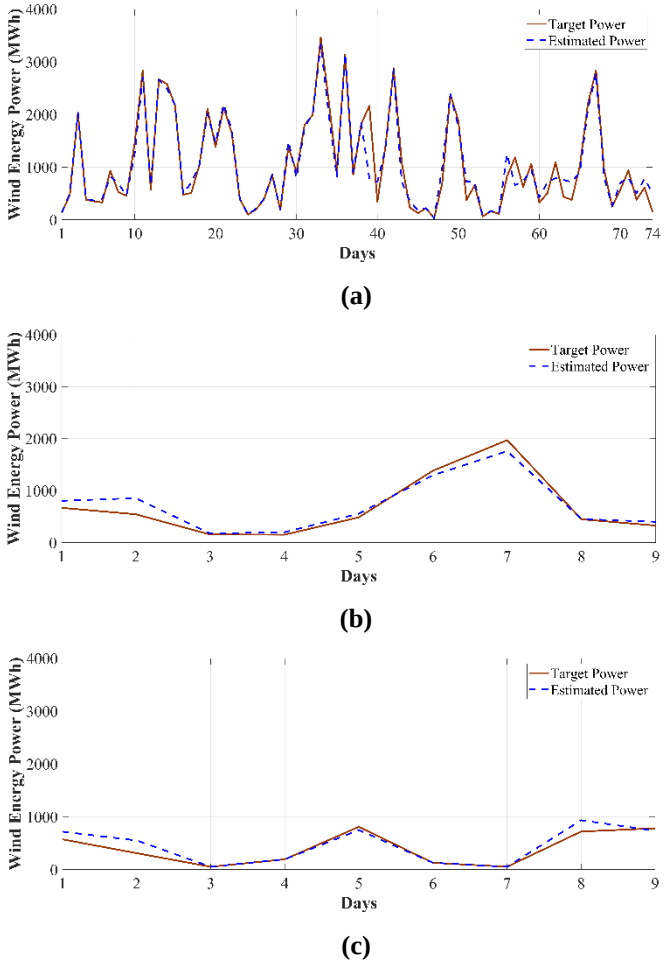

Fig. 13. Prediction results for the ANN model based on three subsets of the dataset: (a) training subset, (b) validation subset, and (c) testing subset.

A comparative analysis of fundamental performance metrics was conducted to comprehensively evaluate and compare the prediction capabilities of the ANN, VMD-ANN, GRU-ANN, and JAYA-ANN hybrid models.

The MAPE values of these models were recorded as 20%, 18.19%, 15.38%, and 12.59%, respectively. These values revealed a gradual improvement in relative prediction accuracy from the basic ANN model to the advanced JAYA-ANN model. The corresponding RMSE values were found to be 28.45 MW, 17.06 MW, 16.11 MW, and 15.10 MW; these values indicate the magnitude of absolute deviations from the observed values and provide a clear measure of each model's overall prediction accuracy. Additionally, the MAE was calculated as 3.34 MW for ANN, 2.20 MW for VMD-ANN, 2.08 MW for GRU-ANN, and 1.77 MW for JAYA-ANN, further illustrating the average prediction errors of the models and confirming the superior prediction consistency of hybrid approaches over the independent ANN model. Figure 17 provides a visual comparison of these model performances, enabling a clear and intuitive understanding of how each approach handles the variability and complexity of wind energy production and highlighting the advantages of hybridization and optimization in improving prediction accuracy. Table 7 provides a detailed evaluation of the prediction performance of four different modelling approaches, including an independent ANN model, along with Hybrid VMD-ANN, GRU-ANN, and JAYA-ANN models. The results presented are based on the dataset used in this study and enable a comprehensive comparison of each model in terms of performance metrics such as accuracy, precision, stability, and generalization ability.

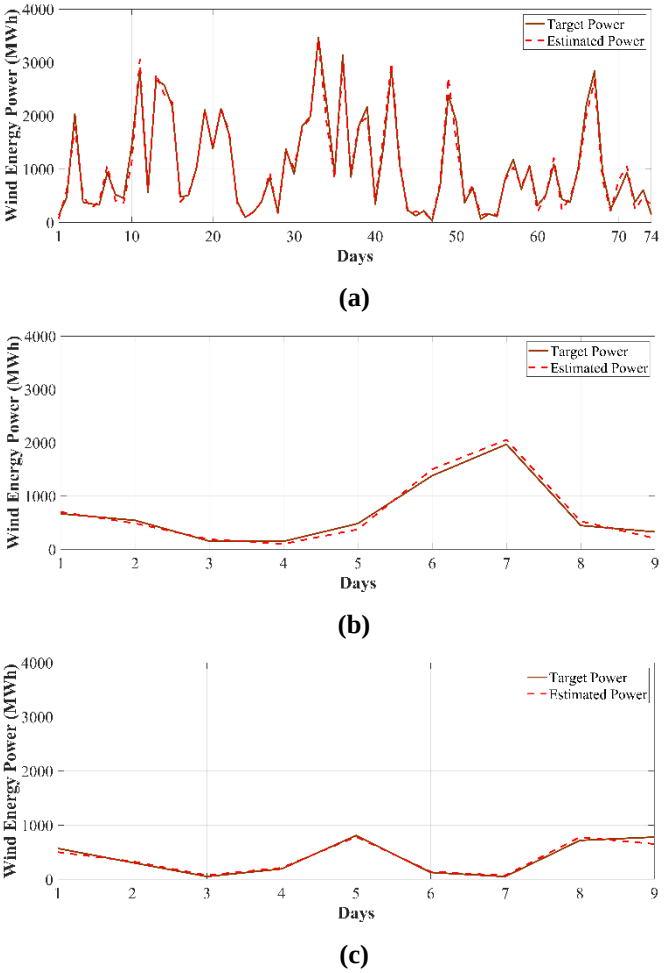

Fig. 14. Prediction results for the VMD-ANN model based on three subsets of the dataset: (a) training subset, (b) validation subset, and (c) testing subset.

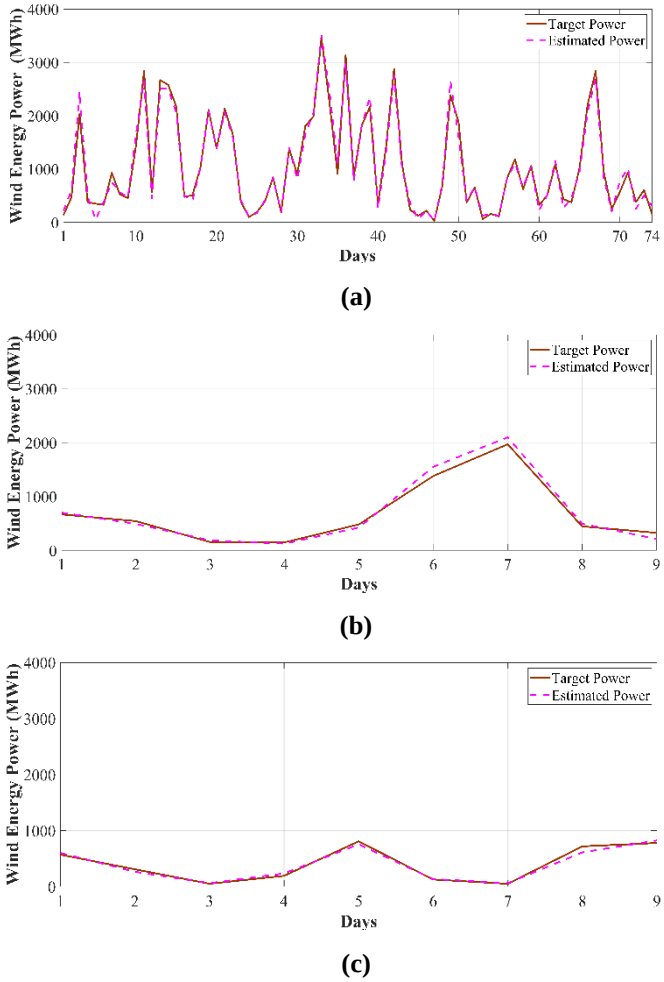

Fig. 15. Prediction results for the GRU-ANN model based on three subsets of the dataset: (a) training subset, (b) validation subset, and (c) testing subset.

The table also includes statistical indicators and error metrics that quantitatively reveal the predictive capacity of each model, allowing for a systematic evaluation of the advantages and limitations of different modelling approaches. In this context, Table 7 not only provides a detailed analysis of the prediction performance specific to the dataset, but also enhances the validity of the methods used in the study and serves as a reference for comparison and model selection in future research.

Table 8 summarizes the input variables, model structures, and performance metrics of different models used for wind energy forecasting in the current literature. The studies provide a comparative assessment using different datasets and forecasting approaches. As the proposed estimation model, the JAYA-ANN model was developed in this study using historical power data, wind direction, temperature, and PM10 parameters. The model's performance was evaluated seasonally, with MAPE found to be 8.36%, RMSE 17.14 MW, and MAE 1.88 MW for the summer season. For the spring period, MAPE was 12.59%, RMSE was 15.10 MW, and MAE was 1.77 MW. These results show that the JAYA-ANN model offers high prediction accuracy compared to other models in the literature, both in minimizing error rates and in adapting to seasonal differences.

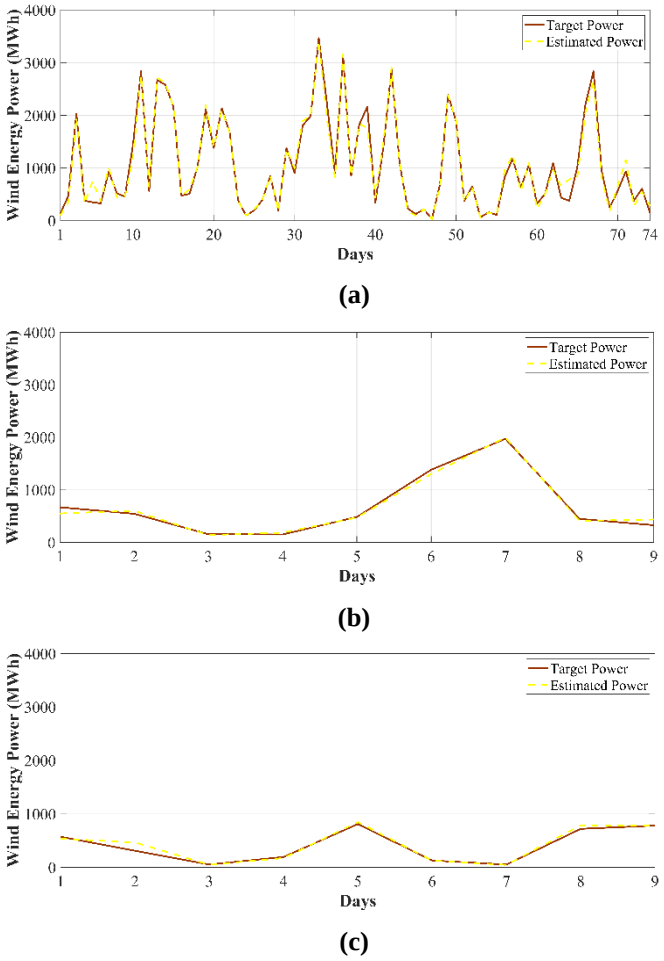

Fig. 16. Prediction results for the JAYA-ANN model based on three subsets of the dataset: (a) training subset, (b) validation subset, and (c) testing subset.

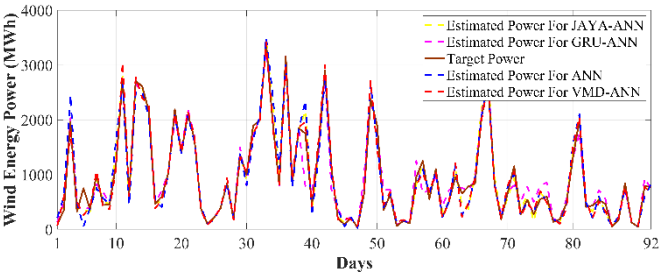

Fig. 17. Prediction results for ANN, VMD-ANN, GRU-ANN, and JAYA-ANN models.

In addition to the obtained performance results, the findings of this study highlight the effectiveness of integrating optimization algorithms with artificial neural network structures for improving wind power forecasting accuracy. The JAYA algorithm, which is based on a simple yet powerful population-based optimization mechanism, plays a significant role in optimizing the weight parameters of the ANN model and enhancing its learning capability. Unlike traditional training approaches that rely solely on gradient descent methods, the JAYA algorithm guides the optimization process by simultaneously approaching the best solution while avoiding the worst solution in the population.

Table 7. MAPE, RMSE, and MEA values according to spring season forecast results

Models	MAPE (%)	RMSE (MW)	MAE (MW)
ANN (training)	20.45	26.38	1.71
VMD-ANN (training)	18.39	15.54	1.39
GRU-ANN (training)	15.81	14.27	1.25
JAYA-ANN (training)	12.76	13.94	1.03
ANN (validation)	19.81	47.22	11.90
VMD-ANN (validation)	17.71	27.74	8.47
GRU-ANN (validation)	14.26	29.40	8.18
JAYA-ANN (validation)	12.45	21.95	6.01
ANN (test)	16.53	40.20	8.76
VMD-ANN (test)	17.02	18.35	4.71
GRU-ANN (test)	13.02	16.36	4.38
JAYA-ANN (test)	11.33	19.93	4.12
ANN (all)	20.00	28.45	3.34
VMD-ANN (all)	18.19	17.06	2.2
GRU-ANN (all)	15.38	16.11	2.08
JAYA-ANN (all)	12.59	15.10	1.77
PRM	41.96	46.65	5.96

This strategy enables the model to achieve improved convergence characteristics by effectively guiding the optimization process toward more optimal solutions while simultaneously reducing the likelihood of the training process becoming trapped in local optima, which is a common limitation encountered in traditional training procedures. As a result, the model is able to learn the underlying patterns of the data more efficiently and reach a more stable solution during the training phase. Furthermore, the incorporation of multiple meteorological parameters, including temperature, wind direction, and PM10 concentration, provides a more comprehensive and realistic representation of the environmental conditions influencing wind energy production, since wind power generation is inherently dependent on complex atmospheric dynamics and the nonlinear interactions among different meteorological variables. Since wind power generation is inherently influenced by atmospheric variability and complex nonlinear relationships among meteorological variables, the inclusion of these parameters enhances the model's ability to capture the dynamic behavior of wind power generation processes. Consequently, the outcomes of this study highlight the potential of hybrid artificial intelligence models as effective and powerful tools for renewable energy forecasting applications. Furthermore, future studies may enhance forecasting performance by incorporating additional meteorological variables, extending the dataset to cover longer time periods, and exploring advanced deep learning architectures combined with optimization algorithms to improve the robustness and generalization capability of wind power prediction models

Table 8. Comparison of predictions made in the literature with the proposed prediction model

Study	Inputs used	Model structure	Error measures
M. Ozturk et al. [34]	Historical power data, wind speed, temperature, relative humidity	ANN	MAPE= %6.46
O.Tasdemir et al [35]	Past power output, wind speed	PSO	RMSE= 44.09 MW
Y. Zhang et al. [36]	Wind Speed and direction	CNN-LSTM	MAE= 8.2 kW
A. Gijon et al. [37]	Wind speed, angle of inclination, rotor speed, torque, and power	ANN	MAPE= %10
A. J. R. Barrera [38]	Temperature, pressure, precipitation, wind	VMD-CNN-GRU	MAE=45.73, RMSE=59.37
Recommended forecast	Historical power data, wind direction, temperature, PM10	JAYA-ANN	Summer period MAPE= %8.36 MAE=1.88 MW RMSE=17.14 MW Spring period MAPE= %12.59 RMSE=15.10 MW MAE=1.77 MW

4. Conclusion

This study analyzes widely used forecasting models for wind power prediction as reported in the literature, with comparisons conducted across different time horizons. Based on an extensive literature review, forecasting methods, prediction intervals, input data types, and error metrics are examined in detail. To ensure a balanced day-ahead supply-demand relationship in wind power systems and to enhance overall system stability, commonly used error evaluation metrics, namely MAPE, RMSE, and MAE, are employed in the evaluation of daily wind power forecasting accuracy.

On the other hand, in this study, the effect of the PM10 parameter on wind power generation is particularly emphasized due to the increasing importance of the impact of air pollution on power generation systems. Analysing the impact of PM10 levels on wind power generation is critical for developing more accurate and reliable forecasting models. Improved forecasting results obtained by including the PM10 parameter enable wind energy power plants to make more accurate and reliable forecasts.

In this study, a hybrid model is developed by combining the JAYA - ANN for wind power forecasting. This hybrid model is compared with GRU and VMD based hybrid ANN models commonly used in the literature. As a result of the comparisons, it was determined that the JAYA-ANN model was superior to the other models in terms of prediction accuracy.

The following inferences were obtained from the estimation results made in the summer period using the data set:

- As a result of the prediction using the ANN, the MAPE, RMSE, and MAE values were obtained as 19.59%, 33.85 MW, and 4.91 MW, respectively. The ANN-based prediction yielded improvements of 41.08%, 49.47%, and 58.97% in MAPE, RMSE, and MAE, respectively, compared to the persistence reference model.

- The hybrid VMD-ANN model achieved MAPE, RMSE, and MAE values of 17.04%, 27.29 MW, and 4.16 MW, in order. Compared to the persistence reference model, the VMD-ANN approach resulted in performance improvements of 48.75% in MAPE, 59.26% in RMSE, and 65.21% in MAE.

- Utilizing the GRU-ANN hybrid model for wind power forecasting resulted in MAPE, RMSE, and MAE values of 14.08%, 25.53 MW, and 3.15 MW, in turn. Compared to the persistence reference model, this hybrid approach led to improvements of 57.65% in MAPE, 61.89% in RMSE, and 73.66% in MAE.

- The JAYA-ANN hybrid model achieved MAPE, RMSE, and MAE values of 8.36%, 17.14 MW, and 1.88 MW, respectively, for wind power forecasting. Compared to the persistence benchmark model, this hybrid approach demonstrated improvements of 74.85% in MAPE, 74.41% in RMSE, and 84.28% in MAE.

The following inferences were obtained from the estimation results made in the spring period using the data set:

- The ANN-based prediction yielded MAPE, RMSE, and MAE values of 20%, 28.45 MW, and 3.34 MW, respectively. Compared to the persistence model, this approach achieved improvements of 52.33%, 39.02%, and 43.96% in MAPE, RMSE, and MAE, respectively.

- The VMD-ANN hybrid model achieved values of 18.19% for MAPE, 17.06 MW for RMSE, and 2.2 MW for MAE. Compared to the persistence model, these results indicate improvements of 56.64%, 63.42%, and 63.08%, respectively.

- The GRU-ANN hybrid model yielded MAPE, RMSE, and MAE values of 15.38%, 16.11 MW, and 2.08 MW, respectively, for wind power forecasting. Relative to the persistence model, it demonstrated improvements of 63.34%, 65.46%, and 65.1% in MAPE, RMSE, and MAE, respectively.

- JAYA-ANN hybrid model yielded MAPE, RMSE, and MAE values of 12.59%, 15.1 MW, and 1.77 MW, respectively. Compared to the persistence benchmark model, this approach achieved improvements of 70% in MAPE, 67.63% in RMSE, and 70.3% in MAE.

As can be clearly seen from the conclusions summarized above, the superior performance of the JAYA-ANN hybrid model over the ANN, VMD-ANN, and GRU-ANN forecasting models in both summer and spring shows that hybrid models can be used effectively in wind power forecasting. Although building and optimizing these models is often a complex process, the results obtained prove that the effort is worthwhile.

In wind power forecasting studies, the provision of data sets constitutes a significant challenge. Therefore, anonymizing the data sets used will facilitate the comparison of similar studies and the sharing of data sets. The absence of any data deficiency in the data set used contributed to the more accurate prediction results.

Future studies may examine the effect of other air pollution parameters and the changes of particulate matter parameters in wind power forecasting. In addition, due to the limited long-term forecasting studies, the long-term performance of hybrid models can also be investigated. The performance of other hybrid models in long-term forecasting can also be analysed. The findings obtained in this study provide valuable information that can be used in the calculation of installation costs and return on investment periods of new wind power plants.

Considering the superior prediction performance of the JAYA-ANN hybrid model, it is recommended that this model be used in new projects and in the improvement of existing systems.

Acknowledgements

The authors declare that no specific funding or institutional support was received for this study.

Author Contributions

Bahtiyar Taşdemir is responsible for conceptualizing the study, validation, data editing, software development, resource provision, and project management. Bahtiyar Taşdemir and Mustafa Yaz jointly contributed to the development of the methodology, formal analysis, research process, preparation of the first draft of the article, review and editing, visualization, and consulting processes. All authors have read and approved the final version of the article.

Conflict of Interest

The author(s) declared no potential conflicts of interest with respect to the research, authorship, and/or publication of this article.

References

[1] A. Gulraiz, S. S. H. Zaidi, M. Ashraf, M. Ali, A. Lashab, J. M. Guerrero, B. Khan, ‘‘Impact of photovoltaic ingress on the performance and stability of low voltage Grid-Connected Microgrids,’’ Results in Engineering, Volume 26, 2025, 105030, ISSN 2590-1230, https://doi.org/10.1016/j.rineng.2025.105030.

[2] Global Wind Report 2024, Accessed: Jan. 14, 2025. [Online]. Available: https://gwec.net/global-wind-report-2024.

[3] S. Hu, Y. Xiang, H. Zhang, S. Xie, J. Li, C. Gu, W. Sun and J. Liu, “Hybrid forecasting method for wind power integrating spatial correlation and corrected numerical weather prediction,” Appl. Energy, vol. 293, p. 116951, Jul. 2021, doi: 10.1016/j.apenergy.2021.116951.

[4] L. Ye, B. Dai, Z. Li, M. Pei, Y. Zhao, and P. Lu, “An ensemble method for short-term wind power prediction considering error correction strategy,” Appl. Energy, vol. 322, p. 119475, Sep. 2022, doi: 10.1016/j.apenergy.2022.119475.

[5] J. Liu, Z. Zhao, J. Ji, and M. Hu, “Research and application of wireless sensor network technology in power transmission and distribution system,” Intelligent and Converged Networks, vol. 1, no. 2, pp. 199–220, Sep. 2020, doi: 10.23919/ICN.2020.0016.

[6] Z. Ma and G. Mei, “A hybrid attention-based deep learning approach for wind power prediction,” Appl. Energy, vol. 323, p. 119608, Oct. 2022, doi: 10.1016/j.apenergy.2022.119608.

[7] X. Zhao, S. Wang, and T. Li, “Review of evaluation criteria and main methods of wind power forecasting,” Energy Procedia, vol. 12, pp. 761–769, 2011, doi: 10.1016/j.egypro.2011.10.102.

[8] S. Hanifi, X. Liu, Z. Lin, and S. Lotfian, “A critical review of wind power forecasting methods—Past, present and future,” Energies (Basel), vol. 13, no. 15, p. 3764, Jul. 2020, doi: 10.3390/en13153764.

[9] Y. Wang, R. Zou, F. Liu, L. Zhang, and Q. Liu, “A review of wind speed and wind power forecasting with deep neural networks,” Appl. Energy, vol. 304, p. 117766, Dec. 2021, doi: 10.1016/j.apenergy.2021.117766.

[10] O. Karakoç and İ. Buğdaycı, “Spatial modeling of chlorophyll-a parameter by Landsat-8 satellite data and deep learning techniques: The case of Lake Mogan”, NOHU J. Eng. Sci., vol. 14, no. 2, pp. 615–629, 2025, doi: 10.28948/ngumuh.1603421.

[11] S. M. Malakouti, “Estimating the output power and wind speed with ML methods: A case study in Texas,” Case Studies in Chemical and Environmental Engineering, vol. 7, p. 100324, Jun. 2023, doi: 10.1016/j.cscee.2023.100324.

[12] X. Gao, W. Guo, C. Mei, J. Sha, Y. Guo and H. Sun, “Short-term wind power forecasting based on SSA-VMD-LSTM,” Energy Reports, vol. 9, pp. 335–344, Oct. 2023, doi: 10.1016/j.egyr.2023.05.181.

[13] B. Xiong, L. Lou, X. Meng, X. Wang, H. Ma and Z. Wang, “Short-term wind power forecasting based on Attention Mechanism and Deep Learning,” Electric Power Systems Research, vol. 206, p. 107776, May 2022, doi: 10.1016/j.epsr.2022.107776.

[14] H. Alkabbani, F. Hourfar, A. Ahmadian, Q. Zhu, A. Almansoori and A. Elkamel, “Machine learning-based time series modelling for large-scale regional wind power forecasting: A case study in Ontario, Canada,” Cleaner Energy Systems, vol. 5, p. 100068, Aug. 2023, doi: 10.1016/j.cles.2023.100068.

[15] J. Zhu, L. Su, and Y. Li, “Wind power forecasting based on new hybrid model with TCN residual modification,” Energy and AI, vol. 10, p. 100199, Nov. 2022, doi: 10.1016/j.egyai.2022.100199.

[16] B. He, L. Ye, M. Pei, P. Lu, B. Dai, Z. Li and K. Wang, “A combined model for short-term wind power forecasting based on the analysis of numerical weather prediction data,” Energy Reports, vol. 8, pp. 929–939, Nov. 2022, doi: 10.1016/j.egyr.2021.10.102.

[17] V. Chandran, C. K. Patil, A. M. Manoharan, A. Ghosh, M. G. Sumithra, A. Karthick, R. Rahim and K. Arun, “Wind power forecasting based on time series model using deep machine learning algorithms,” Mater. Today Proc., vol. 47, pp. 115–126, 2021, doi: 10.1016/j.matpr.2021.03.728.

[18] V. Singh, “Application of artificial neural networks for predicting generated wind power,” International Journal of Advanced Computer Science and Applications, vol. 7, no. 3, 2016, doi: 10.14569/IJACSA.2016.070336.

[19] A. Sharkawy, “Principle of neural network and its main types: Review,” Journal of Advances in Applied & Computational Mathematics, vol. 7, pp. 8–19, Aug.

2020, doi: 10.15377/2409-5761.2020.07.2.

[20] A. D. Rasamoelina, F. Adjailia, and P. Sincak, "A review of activation function for artificial neural network," in Proc. 2020 IEEE 18th World Symposium on Applied Machine Intelligence and Informatics (SAMI), Jan. 2020, pp. 281–286, doi: 10.1109/SAMI48414.2020.9108717.

[21] R. Rojas, Neural Networks: A Systematic Introduction. Berlin, 1996.

[22] T. Saraç, "Estimating software project duration using artificial neural networks," Türkiye, 2005.

[23] R. Venkata Rao, "Jaya: A simple and new optimization algorithm for solving constrained and unconstrained optimization problems," International Journal of Industrial Engineering Computations, pp. 19–34, 2016, doi: 10.5267/j.ijiec.2015.8.004.

[24] Z. He and F. Tong, "Residual RNN models with pruning for digital predistortion of RF power amplifiers," IEEE Trans. Veh. Technol., vol. 71, no. 9, pp. 9735, 2022.

[25] J. Chung, C. Gulcehre, K. Cho, and Y. Bengio, "Empirical evaluation of gated recurrent neural networks on sequence modeling," arXiv preprint, arXiv:1412.3555, 2014.

[26] A. Sherstinsky, "Fundamentals of recurrent neural network (RNN) and long short-term memory (LSTM) network," Physica D: Nonlinear Phenomena, vol. 404, p. 132306, 2020, doi: 10.1016/j.physd.2019.132306.

[27] X. Wang, G. Xie, W. Liu and Yang Gao, "A long-term vertical displacement prediction method of concrete bridges based on meteorological shared data and optimized GRU model," Measurement, vol. 253, Part D, p. 117811, 2025, doi: 10.1016/j.measurement.2025.117811.

[28] K. Dragomiretskiy and D. Zosso, "Variational mode decomposition," IEEE Trans. Signal Process., vol. 62, pp. 531–544, 2014.

[29] M. Fang, F. Zhang, Y. Yang, R. Tao, R. Xiao and D. Zhu, "The influence of optimization algorithm on the signal prediction accuracy of VMD-LSTM for the pumped storage hydropower unit," J. Energy Storage Mater., vol. 78, p. 110187, 2024.

[30] H. Li, S. Li, J. Sun, B. Huang, J. Zhang and M. Gao, "Ultrasound signal processing based on joint GWO-VMD wavelet threshold functions," Measurement, vol. 226, p. 114143, 2024.

[31] X. Yan and M. Jia, "Application of CSA-VMD and optimal scale morphological slice bispectrum in enhancing outer race fault detection of rolling element bearings," Mech. Syst. Signal Process., vol. 122, pp. 56–86, 2019.

[32] R. Perez, S. Kivalov, J. Schlemmer, K. Hemker, D. Renne and T. Hoff, "Validation of short and medium term operational solar radiation forecasts in the US," Solar Energy, vol. 84, pp. 2161–2172, 2010. https://doi.org/10.1016/j.solener.2010.08.014.

[33] O.Taşdemir, "Photovoltaic Power Prediction with Teaching Learning Based Optimization Algorithm," Gazi University Journal of Science Part A: Engineering and Innovation, 11(4), 780-791, 2024. https://doi.org/10.54287/gujsa.1581828.

[34] M. Öztürk, R. Kayabaşı and O. Taşdemir, "Kirşehir'in rüzgar enerjisi potansiyeli ve iç anadolu bölgesi kurulu rüzgar enerjisi santrallerinin güç analizi," Kahramanmaraş Sütçü İmam Üniversitesi Mühendislik Bilimleri Dergisi, 28(1), 189-201. https://doi.org/10.17780/ksujes.1533576.

[35] O. Taşdemir, İ. F. Tepe ve E. Irmak, "PSO algoritması ile mevsimsel rüzgar enerjisi tahminlerinin optimizasyonu, " 2024 6. Küresel Güç, Enerji ve İletişim Konferansı (GPECOM) , Budapeşte, Macaristan, 2024, ss. 543-548, doi: 10.1109/GPECOM61896.2024.10582566.

[36] Y. Zhang, H. Su, R. Wang, J. Deng, Y. Wang, W. Guo and R. Li, "Short-term forecast method of wind power output based on multi-scale CNN-LSTM in extreme weather, " International Journal of Electrical Power & Energy Systems, Volume 172, 2025, 111191, ISSN 0142-0615, https://doi.org/10.1016/j.ijepes.2025.111191.

[37] A. Gijón, A. P. Goitia, E. Perea, M. M. Solana and J. G. Romero, "Prediction of wind turbines power with physics-informed neural networks and evidential uncertainty quantification, " Engineering Applications of Artificial Intelligence, Volume 164, Part B, 2026, 113331, ISSN 0952-1976, https://doi.org/10.1016/j.engappai.2025.113331.

[38] A. J. R. Barrera, A. E. Sipols, A. P. Garcia and M. A. L. Carmona, "Short-term wind power forecasting integrating wake effect modeling with variational mode decomposition enhanced deep learning architectures, " Energy Conversion and Management, Volume 348, Part C, 2026, 120738, ISSN 0196-8904, https://doi.org/10.1016/j.enconman.2025.120738.